Korean J. Chem. Eng., **23**(5), 819-826 (2006)

Agglomeration behavior of anhydrous L-ornithine-L-aspatate crystals during semi-batch drowning-out crystallization

Woochan Hyung, Yehoon Kim, Seungjoo Haam† and Kee-Kahb Koo*

Department of Chemical Engineering, Yonsei University, Seoul 120-749, Korea
*Department of Chemical and Biomolecular Engineering, Sogang University, Seoul 121-742, Korea
(*Received 6 February 2006 • accepted 10 May 2006*)

Abstract–Crystallization of L-ornithine-L-aspartate (LOLA) by drowning out was carried out to produce the anhydrous form of agglomerates. The primary crystal size in the agglomerate remained unchanged after completion of the crystallization. The LOLA aqueous solution introduced into the system was immediately dispersed and cluster coagulated on the surface of the crystals. On the surface of the crystals, a cluster reached critical nuclei size, nucleated and intergrowth to form agglomerates. It was proposed that a spherical agglomeration occurred during secondary nucleation by coagulation model and intergrowth. The agglomerates size and size distribution were varied with the process parameters. The agglomerate sizes of LOLA crystals appeared to be ruled not only by secondary nucleation rate but also by the mass of suspended agglomerates. Moreover, the agglomeration rates of fine particles were higher than the agglomeration rates of large agglomerates. Using these properties, the uniform agglomerates size distribution could be obtained.

Key words: Drowning-Out, L-Ornithine-L-Aspartate, Pseudopolymorph, Agglomeration, Impurity

INTRODUCTION

Crystallization by drowning out is widely used for the separation of pharmaceutical products and biomaterials in industrial processes [Myerson, 1993; Wolfgang, 1999]. In drowning out crystallization, the supersaturation is generated by addition of an antisolvent which reduces the solubility of the solute. This method is rather than the evaporative or cooling crystallization for high soluble material which has weak temperature dependence on solubility [David et al., 1997]. In particular, it is also suitable for separation of heat labile material because crystallization can occur at lower temperature. However, it needs to handle large quantities of antisolvent in order to obtain the desirable yield and impurities incorporated into the crystal, and those are the main disadvantage of this method. In pharmaceutical industries, crystal size and shape have an effect on solid-liquid separation and so purity, and on downstream process, such as capsule-filling and tablet-making for preparing solid dosage forms [Chulia et al., 1994]. According to the study of the drowning-out crystallization, the addition rate of antisolvent and agitation rate were found to be significant factors in determining the crystal size and shape [Charmolue and Rousseau, 1991]. It was suggested that the purity may be related to size and shape of product crystals. The crystal size and the shape have been also shown to be important factors in flowability and compressibility [Szabó-Révész et al., 2001]. Therefore, it is essential to understand the characteristics of crystals with the change of operational variables for the effective crystallization by drowning out.

L-ornithine-L-aspartate (LOLA) is a complex of the basic amino acid (L-ornithine) with acidic amino acid (L-aspartic acid). L-ornithine ($C_5H_{12}N_3O_2$), an antidote to ammonia in the blood, is known to play an important role in the urea production of the ornithine cycle in the living body. L-aspartic acid ($C_4H_7NO_4$) also plays a role as an amine-donor in the ornithine cycle and thus used for preventing hepatic disturbance. Their simultaneous administration in the form of LOLA has proven to be more effective in reducing blood ammonia concentration in patients with acute liver failure [Rees et al., 2000; Rose et al., 1998, 1999; Vogels et al., 1997]. We previously reported the effect of operating conditions on the polymorphs of LOLA during drowning out crystallization [Kim et al., 2003]. It is important in this method to make the speed of addition of the aqueous solution and control the temperature since the undesired polymorphs, hydrate, was obtained. The hydrate of LOLA is not suitable for commercial purpose because of coloration and swelling during storage for a long period of time, while the anhydrous form does not have such problems. When methanol was added into the LOLA aqueous solution, the anhydrous form was only obtained at temperature above 60 °C. On the other hand, when the LOLA aqueous solution was added into methanol, the crystal form depended not only on the operating temperature but also on the feeding rate of the LOLA aqueous and methanol concentration. In addition, it was found that the generation and the redissolution of the initial precipitates occurred simultaneously in early feeding stage of aqueous LOLA solution into the antisolvent. At low feed concentration all of the initial precipitates of LOLA dissolved and nucleation occurred again with induction period. Hence the nucleation of LOLA at low feed concentration could be explained by the primary nucleation theory via induction period measurement. At the high feed concentration, however, an enormous shower of nuclei during the feeding was observed. Thus, the presence of precipitates reduced the induction period as seeds by the catastrophic secondary nucleation. This mechanism offered the formation of a certain type of agglomerates those which appear to be formed around a crystal not by the capture of other smaller crystals but by the appearance of new crystals very close to

†To whom correspondence should be addressed.
E-mail: haam@yonsei.ac.kr

the surface of the original crystal [Kim et al., 2006].

Two types of secondary growth of particles can be differentiated according to the intensity of interparticle force: aggregation for weak force such as van der Waals force and agglomeration for strong force such as chemical bond. Agglomeration may alter the particle size, physical properties, and surface properties to make the agglomerated particles more useful. For example, agglomeration is beneficially employed to impart desirable flow properties, to reduce dusting hazards and losses, to facilitate the recovery of fines, to prevent the segregation of a component, to densify, and to create definite sizes and shapes [Kawashima et al., 1982]. Recently, crystals of small size (<10 μm) are often needed in biomaterial or pharmaceutical industry due to their high bioavailability and dissolution kinetics. However, their downstream processing may be difficult such as filtration, handling and storage. Therefore, the production of spherical agglomerates of pharmaceutical compound crystals has gain great attention, because the modification of the crystal habit can change the bulk density, flowability, compactibility and stability [Brittain, 1999]. Moreover, the formation of the spherical crystal agglomerates is important for preparing the solid dosage forms by capsule filling and tablet making.

In the present study, agglomeration of LOLA was investigated for controlling the size and crystal size distribution [Kim et al., 2003; Kage et al., 1999; Choe et al., 2003]. The process parameters including operating temperature, feed concentration, agitation speed, and feeding rate on agglomerations determining the agglomeration behavior were fully tested in a semibatch drowning out crystallizer. The experimental conditions were limited to the range of parameters in which only anhydrous form was obtained.

EXPERIMENTAL

1. Materials and Experimental Procedure

LOLA ($C_5H_{13}N_3O_2^+ \cdot C_4H_6NO_4^-$, MW 265.3) was supplied by Sigma Chemical Co. and deionized water (conductance less than 4 μs/cm) and methanol (Merck, ±99.8 mol%) were used without further purification.

The crystallization experiments of LOLA were conducted by adding LOLA aqueous solution into an antisolvent, methanol. As the LOLA aqueous solution with a constant flow rate was added into the bulk methanol phase, a high supersatured state of LOLA complex was immediately created and the anhydrous form of LOLA crystals tended to be nucleated. As the amount of LOLA aqueous solution increased, the agglomeration of crystals occurred. During the experiment, the supersaturation was determined by monitoring the initial feed concentration of LOLA. The crystallization temperature was controlled at constant 40, 50 and 60 °C. The feeding rate and the feed concentration of LOLA solution were varied from 0.1 to 1.0 g/min and from 0.5 to 2.0 mol/l, respectively. The total amount of LOLA aqueous solution used was 30 g. The agitation speed was varied from 300 to 700 rpm. At these conditions, no particle breakage was observed. The experimental setup and procedure are detailed elsewhere [Kim et al., 2001, 2003]. After reaching the saturation, the equilibrium state, 5 ml of suspension was also sampled from the crystallizer using a micropipette. The size distribution of the crystals dispersed in a methanol solution was measured by using a particle size analyzer (HIAC 9703). To investigate the crystal structure and morphology, the crystals were filtered and dried for 24 hr at 50 °C. The surface morphology of agglomerated crystals was observed under a scanning electron microscope (SEM). Each polymorph was identified using a powder X-ray diffractometer (Rigaku, D/MAX-2500H). To characterize the products, crystal impurity and methanol content were measured by gas chromatography (HP 4890D).

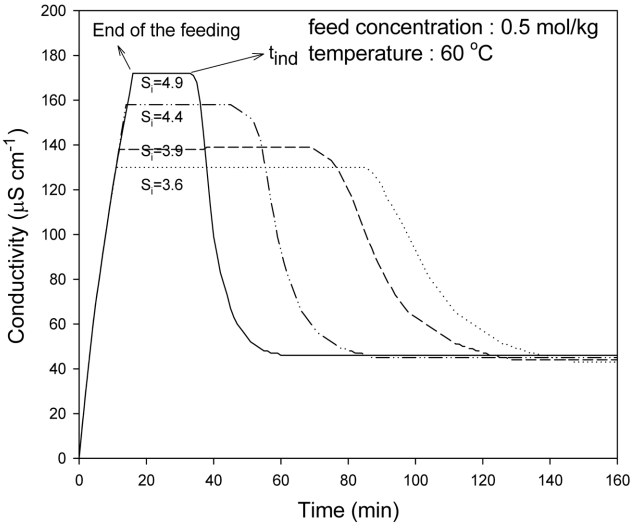

Fig. 1. Evolution of conductivity at different initial supersaturation ratios.

RESULTS AND DISCUSSION

1. Evolution of LOLA Crystal Agglomerate

Crystal agglomeration has been verified not only from analysis of crystal size distribution but also from microscopic observation. The time dependence of solution conductivity was measured and combined with determination of the crystal number and the size formed during crystallization. In Fig. 1, desupersaturation curves provide information about the course of precipitation: crystal formation by nucleation and subsequent crystal growth. As shown in Fig. 2, the morphology of the primary crystals was needle type, showing the characteristic morphology of the anhydrous form of LOLA. The needle type primary crystals were agglomerated and then the size of agglomerates was increased during the feeding time. The size of the primary crystals in the agglomerate was 15-20 μm and remained unchanged after completion of the crystallization. Therefore, the results indicated that the crystal size was dominantly influenced by the agglomeration. As we previously reported, the secondary nucleation occurred by coagulation of clusters in the surface of crystal, followed by intergrowth of secondary nuclei for agglomeration [Kim et al., 2006]. Intergrowth occurs when nonparticulate material is deposited on the surface of a particle. During the precipitation in solution, the nonparticulate material is normally an ionic diffusion to, and reacting on the surface of a crystal. Most practical situations deal with precipitates consisting of large numbers of crystals with sizes on the order of a few micrometers. Under the shear force with agitation, the agglomerates were spheronized and compacted. This agglomeration mechanism was termed spherical agglomeration (SA) process as suggested in Fig. 2.

2. Progress of Crystallization

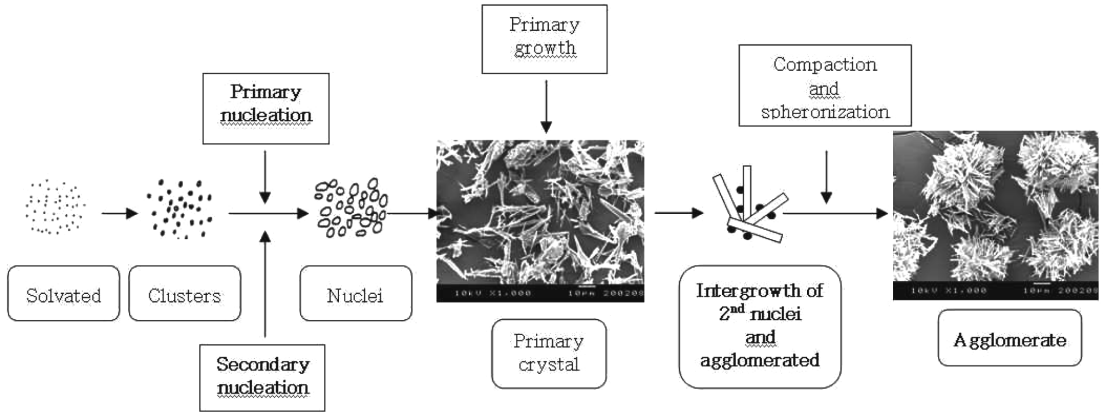

Fig. 2. Proposed crystallization mechanism of LOLA in drowning out.

For a constant volume isothermal batch crystallizer, a supersaturation balance can be written as

$$-\frac{d\Delta c}{dt} = k_b M_t^j \Delta c^b + k_G \Delta c^g \quad (1)$$

In the RHS of Eq. (1), the first term is nucleation rate and the last one is growth rate. In general, it is difficult to predict the secondary nucleation rates due to the various competing mechanisms (growth, secondary nucleation and agglomeration). However, it could be assumed in this process that all monocrystals have the same shape and size that they do not change during agglomeration. After induction period, the precipitates were immediately measured less than 1 min after the nucleation. Growth of crystal was rapid at the beginning and the mean and the size of monocrystal did not change. This means that the period of agglomeration and secondary nucleation occurred simultaneously. Therefore, the change of mass could be obtained from secondary nucleation with constant monocrystal size. Then, Eq. (1) can be modified as

$$-\frac{d\Delta C}{dt} = K M_T^j \Delta c^b \quad (2)$$

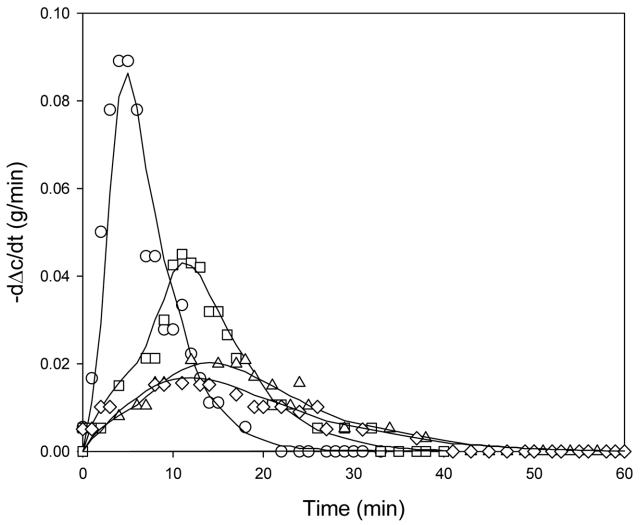

Fig. 3. Desupersaturation rate curve (○: S_i=4.9, □: S_i=4.4, △: S_i=3.9, ◇: S_i=3.6, —: calculated curves of Eq. (4)-(12) using fitted parameter, b=1.5, j=0.7).

From the measurement of magma density change according to the supersaturation, the experimental data of desupersaturation rate

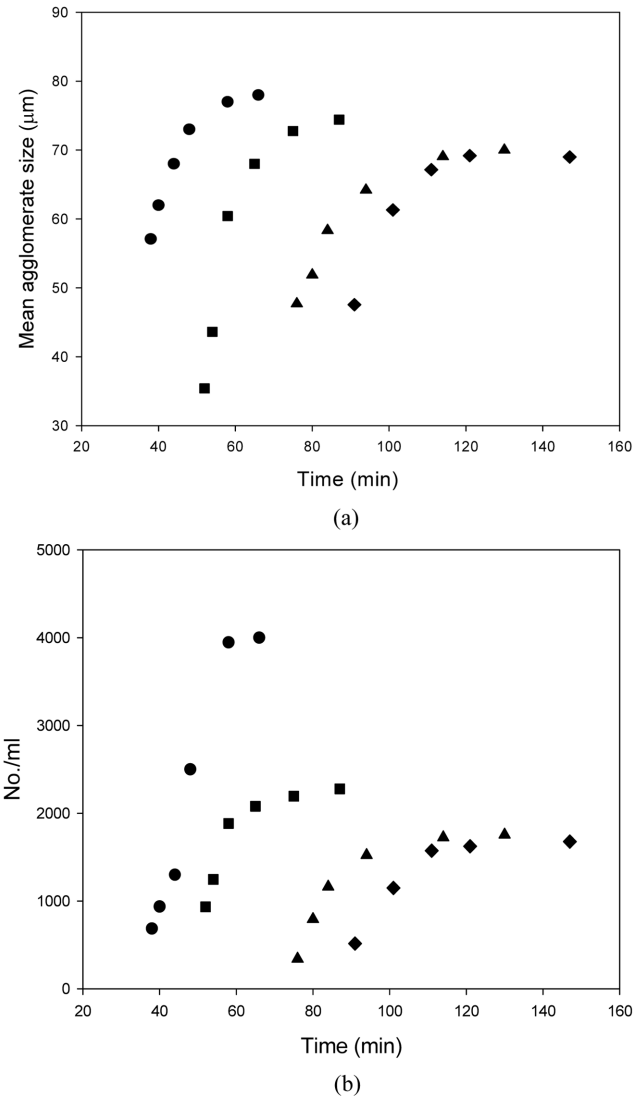

Fig. 4. (a) The mean size and (b) the number of the agglomerates of LOLA crystals (●: S_i=4.9, ■: S_i=4.4, ▲: S_i=3.9, ◆: S_i=3.6).

were fitted with Eq. (2). As shown in Fig. 3, the experimental data were in a good agreement with the calculated values and Eq. (2) seemed to be reasonable in this process. Based on our previous studies, we observed that all secondary nuclei were created around the crystals and the overall nucleation rate in the crystallizer was dependent upon the total surface area of the suspended crystals. However, the suspension density's power in Eq. (2), j, was not 1.0 but 0.7 because the total surface area decreased with agglomeration.

The effect of the supersaturation on the agglomeration was investigated. The mean size and number of the agglomerates were plotted as a function of residence time at various initial supersaturations in Fig. 4. As shown in Fig. 4(a), the mean agglomerate size was 70 μm at low initial supersaturation (S_i=3.6 and 3.9) but at higher supersaturation, the agglomerates larger than 70 μm were observed because of high agglomeration probability for the successful intergrowth of the crystals due to the increased secondary nucleation rate at this high supersaturation. If all secondary nuclei attached on the present crystal, the agglomerates number did not change. However, Fig. 4(b) showed that the agglomerates number increased with increase of supersaturation. It means that the secondary nuclei may be removed to the bulk by the shearing action of the fluid or can also attach themselves on the parent crystal in which case polycrystalline agglomerates are produced. Therefore, this makes bimodal curves of agglomerate size distribution as shown in Fig. 5. The evolution of size distributions of LOLA agglomerates was illustrated in Fig. 5. The monocrystals were well represented by the first population peak within the size of range 0-20 μm and the CSD shifted to right due to agglomeration. As a result, the development of a second peak at larger sizes in the size distribution was the result of agglomeration rather than the presence of larger single crystals as shown in Fig. 2. After the desupersaturation was ended, the agglomeration was terminated. This proved that supersaturation and secondary nuclei were necessary to consolidate the agglomerates of LOLA. In this agglomeration process, the recovery rate of the product ranged from 90-95%. We also confirmed that no polymorphic change of the primary crystals was observed in any of the agglomerates by the powder

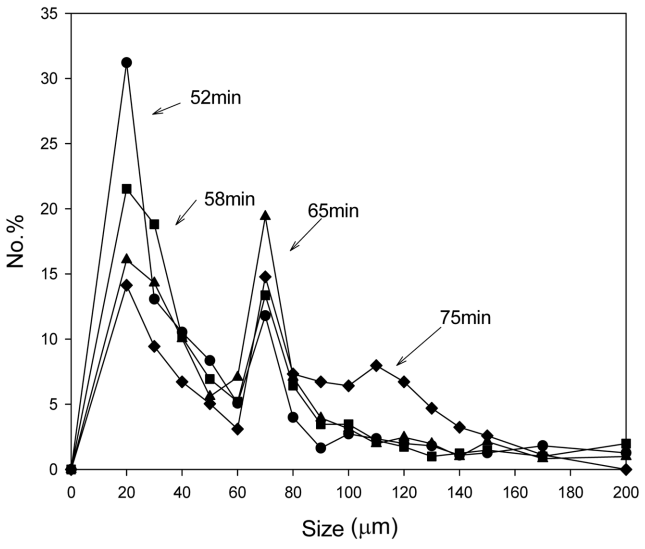

Fig. 5. The change of agglomerate size distribution at S_i=4.4 (●: 52 min, ■: 58 min, ▲: 65 min, ◆: 75 min).

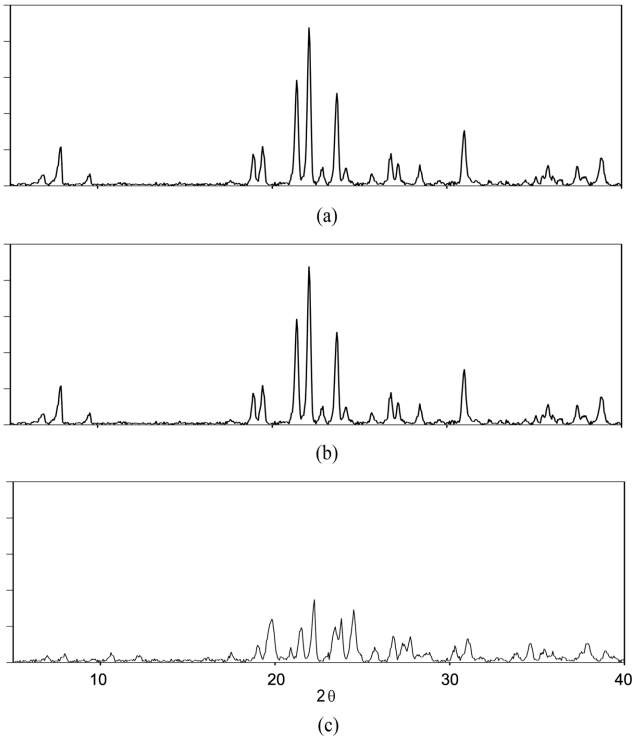

Fig. 6. Powder X-ray diffraction patterns of agglomerates and primary crystals.
(a) anhydrate, (b) anhydrate produced after completion of agglomeration, (c) hydrate

X-ray diffraction patterns of the primary crystals consisting of agglomerates as shown in Fig. 6.

3. Agglomeration Mechanism in Semi-batch Crystallizer

The agglomeration mechanism was investigated in the semi-batch crystallizer with the suspended agglomerates. Two main parameters: the agglomerate mass and the feed concentration were studied. The aqueous LOLA solution was introduced to the semibatch crystallizer with the suspended agglomerates for spherical agglomeration by secondary nucleation with different agglomerate mass (0.25, 0.5 and 0.75 g, respectively) and feed concentrations (0.2 and 0.5 mol LOLA/kg H_2O). As shown in Fig. 7, after the addition of the aqueous LOLA solution, the agglomeration began immediately, and the spherically agglomerated crystals gradually formed by coalescence of dispersed crystals until the end of feeding with saturated concentration. It is obvious that the increase of the feed concentration leads to an acceleration of the agglomerate rate by increasing secondary nucleation. The changes in the total number of different sized agglomerates are shown in Fig. 8. Indeed, the growth had almost no effect on the total number of agglomerates, and only agglomeration could lead to a decrease in total number, N. It could also be seen that agglomeration was strongly dependent on feed concentration. The total number of agglomerates remained constant after feeding was ended. Because the LOLA concentration was very close to equilibrium value, the agglomeration rate, similar to the growth rate, was negligible at zero supersaturation but was appreciable at high supersaturation. The evolution of agglomerates is also shown in Fig. 9. The number of monocrystals was reduced and the size of agglomerates was increased by feeding the aqueous LOLA

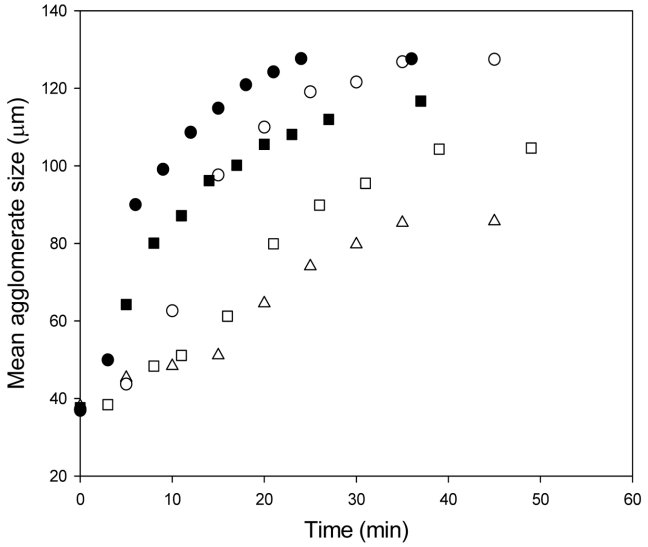

Fig. 7. Increase of agglomerate size by additional feeding of aqueous LOLA solution (●: 0.5 mol LOLA/kg H_2O, 0.25 g of suspended agglomerates, ■: 0.5 mol LOLA/kg H_2O, 0.5 g, ○: 0.2 mol LOLA/kg H_2O, 0.25 g, □: 0.2 mol LOLA/kg H_2O, 0.5 g, △: 0.2 mol LOLA/kg H_2O, 0.75 g).

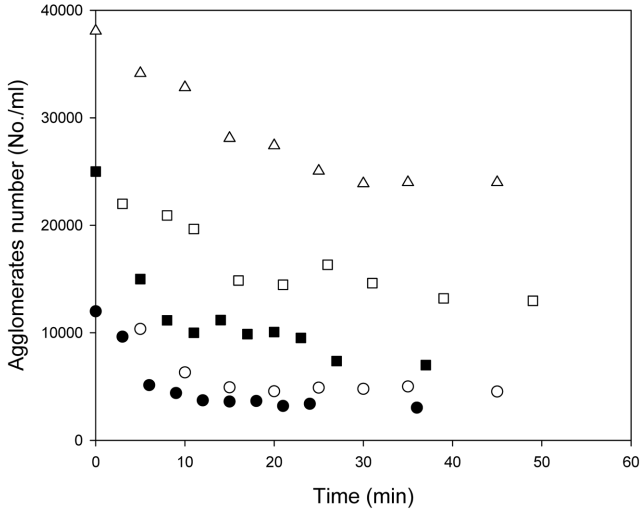

Fig. 8. Decrease of agglomerates number by additional feeding of LOLA aqueous solution (●: 0.5 mol LOLA/kg H_2O, 0.25 g of suspended agglomerates, ■: 0.5 mol LOLA/kg H_2O, 0.5 g, ○: 0.2 mol LOLA/kg H_2O, 0.25 g, □: 0.2 mol LOLA/kg H_2O, 0.5 g, △: 0.2 mol LOLA/kg H_2O, 0.75 g).

solution. As mentioned earlier, the size of primary crystals in the agglomerates remained unchanged after completing the crystallization. Although the larger primary crystals were also found exceptionally, it was unusual to find the larger primary crystals. However, the possibility of primary crystal growth should be considered for the evaluation of agglomerates size distribution. In case of spherical agglomerates of steroid, it was found that the size of primary crystals increased until the dispersing medium was saturated with the bridging liquid. The results indicated that the growth rate of primary crystals increased with an increase in the temperature and a reduction in the agitation speed. During this period, the agglomeration rate can be calculated as a function of time. In the present experiments, the degree of agglomeration was defined from the ratio

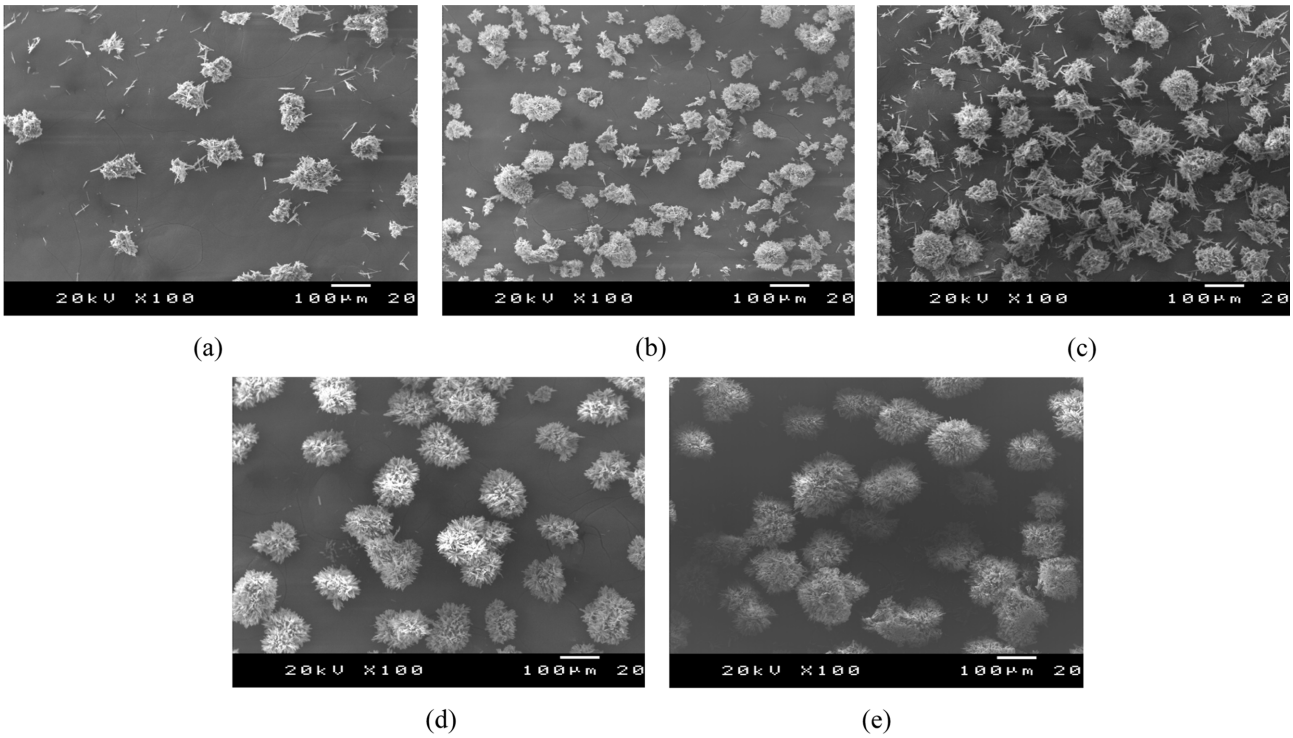

Fig. 9. SEM photographs of LOLA agglomerates at 0.5 mol LOLA/kg H_2O and 0.25 g of suspended agglomerates.
(a) initial agglomerates, (b) 5 min, (c) 10 min, (d) 20 min, (e) 40 min.

Table 1. Agglomeration rate (–dN/dt) according to the feed concentration

Feed concentration	Agglomerate mass	Agglomeration rate*
0.2 mol LOLA/kg H_2O	0.25 g	123
0.2 mol LOLA/kg H_2O	0.5 g	194
0.2 mol LOLA/kg H_2O	0.75 g	282
0.5 mol LOLA/kg H_2O	0.25 g	238
0.5 mol LOLA/kg H_2O	0.5 g	534

*Agglomeration rate=$(N_s - N_f)$/feeding time

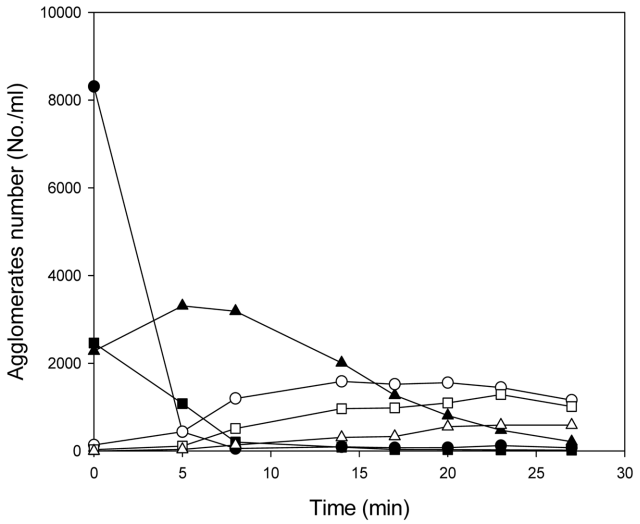

Fig. 10. Size dependent agglomeration (●: 20 μm, ■: 40 μm, ▲: 70 μm, ○: 100 μm, □: 120 μm, △: 150 μm).

between the number of agglomerates at the beginning and at the end of the run, N_s/N_f. With this ratio, the agglomeration rate could be calculated which was presented in Table 1. The total number of agglomerates at the end of the experiment was found to be lower than the initial value for all experiments where the small sized agglomerates were used, indicating that agglomeration was an important mechanism in the process as shown in Fig. 10. The agglomeration rate was defined as the decreasing rate of particle number since no monocrystal was observed during experiments. As a result, the agglomeration rate was increased with increase in the suspended agglomerates mass and feed concentration as listed in Table 1. Consequently, the result confirmed that the agglomeration increased by higher secondary nucleation rate and larger surface area of the suspended agglomerates as suggested in agglomeration mechanism.

The crystal size distribution (CSD) presented in Fig. 11 also give an interesting insight into the agglomeration mechanism. For instance, the fast and complete disappearance of the fine particles at the beginning of the process could signify the higher agglomeration rates of fine particles than the agglomeration rates of large agglomerates. General agglomeration models promoting agglomeration between the largest particles are unable to describe spherical agglomeration phenomena. This agglomeration mechanism appears to be formed around a crystal not by the capture of other smaller crystals but by the appearance of new crystals very close to the surface of the original crystal.

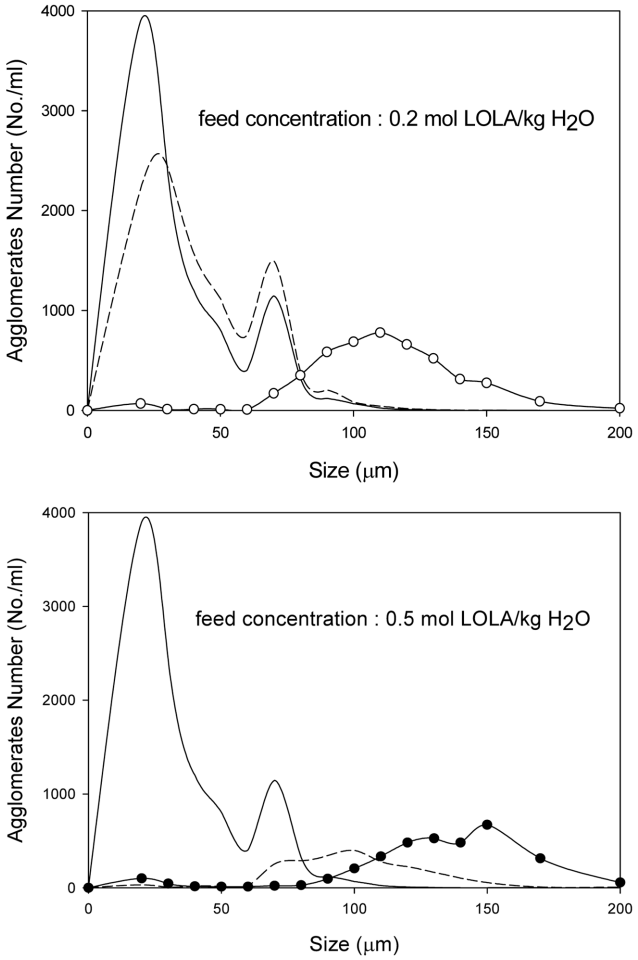

Fig. 11. The change of agglomerate size distribution (—: initial agglomerates, —: feeding time (15 min), ●, ○: feeding time (30 min)).

4. Characterization of Products

The spherical agglomerates have good flowability and compressibility. However, solvent could easily be trapped between the individual crystals which formed agglomerates. As the agglomerates was smaller, contained fewer crystals, and were accompanied by less entrapped methanol. Table 2 indicated that the purity of final products correlated with the size of the agglomerates. Agglomerates of the higher impurity were produced when the mean size of agglomerates increased. When the mean size of agglomerates was increased from 30 μm to 147 μm, the methanol content was increased from 163 to 400 ppm. The methanol content in agglomerates having different morphology was also shown in Table 2. The methanol content was two times higher for hydrate than for anhydrate in the same agglomerates size. It indicated that the anhydrate was preferable in terms of purity. Purity, size and morphology appeared to be closely related but crystal flowability and impurity of agglomerates are restricted conditions each other. Thus, the optimum condition could be obtained through a compromise between flowability and impurity.

5. Control of CSD Using Semibatch Crystallizer

As we discussed earlier, agglomeration rate and the final size of the agglomerates depend on secondary nucleation rate and surface area of the suspended crystals. Moreover, agglomeration rates of

Table 2. Effect of agglomerate size on the purity of LOLA crystals

Form	Hydrate	Anhydrate	Anhydrate	Anhydrate	Anhydrate	Anhydrate
Mean size (μm)	120	30	41	76	95	147
MeOH content (mg/LOLA kg)	818	163	179	221	310	400

fine particles are higher than agglomeration rates of large agglomerates. Using these properties, typical results concerning the evolution of CSD with additional feeding time could be obtained. The fast and complete disappearance of the fine particles at the beginning of the process could make bimodal curve to monocurve as shown in Fig. 11. As a result, the bimodal curve was developed to the monocurve by controlling the addition of aqueous LOLA solution.

CONCLUSION

The agglomeration mechanism of LOLA showed a certain type of agglomerate formation: agglomerates to be formed around a crystal not by the capture of other smaller crystals but by the appearance of new crystals very close to the surface of the original crystal. The nuclei can also attach themselves on the parent crystal in which case we have the formation of polycrystalline agglomerate. It was proposed that a spherical agglomeration occurred during secondary nucleation by coagulation model and intergrowth. The LOLA aqueous solution introduced into the system is immediately dispersed and cluster coagulated on the surface of the crystals. On the surface of the crystals, a cluster reached critical nuclei size and nucleated and intergrowth and formed agglomerates.

The agglomerates size and size distribution varied with the process parameters. The agglomerate sizes of LOLA crystals appeared to be ruled by secondary nucleation rate but also by the mass of suspended agglomerates. Moreover, the agglomeration rates of fine particles are higher than the agglomeration rates of large agglomerates. Using these properties, the uniform agglomerates size distribution could be obtained.

Finally, the present results showed the probability for controlling the morphology and crystal size in drowning out crystallization and would give valuable information on the modeling of crystallization in industrial field. In addition, we convinced that our attempt for analysis of crystallization mechanism would be useful for understanding the crystallization of other complex organic molecule such as protein, organic complex or organic-inorganic complex.

NOMENCLATURE

C : concentration [mol/kg]
c^* : solubility [mol/kg]
c_0 : total feed concentration [mol/kg]
M_T : mass of solid [kg]
N : number of particle
S : supersaturation ratio
T : absolute temperature [K]
t : time [s]
T_{ind} : induction period [s]
x : molar fraction
x_a : the antisolvent-to-water ratio

Subscripts

i, j : density of crystal [kg m^{-3}]
m : NRTL binary interaction energy parameter
T : the dissociation degree of an electrolyte [$=\Lambda/\Lambda_0$]
w : molal conductance [S/cm mol]
Limiting molal conductance [S/cm^2/mol]

REFERENCES

Brittain, H. G., *Polymorphism in pharmaceutical solids*, Marcel Dekker, New York (1999).

Charmolue, H. and Rousseau, R. W., "L-Serine obtained by methanol addition in batch crystallization," *AIChE J.*, **37**, 1121 (1991).

Choe, J., Kwon, Y. and Kim, Y., "Micromixer as a continuous flow reactor for the synthesis of a pharmaceutical intermediate," *Korean J. Chem. Eng.*, **20**, 268 (2003).

Chulia, D., Deleuil, M. and Pourcelot, Y., *Powder technology and pharmaceutical processes*, Elsevier, Amsterdam (1994).

David, A. B., Susan, R. D. and Ka, M. N., "Synthesis of drowning-out crystallization-based separations," *AIChE J.*, **43**, 91 (1997).

Kage, H., Dohzaki, M. and Ogura, H., "Powder coating efficiency of small particles and their agglomeration in circulating fluidized bed," *Korean J. Chem. Eng.*, **16**, 630 (1999).

Kawashima, Y., Okumura, M. and Takenaka, H., "Spherical crystallization: Direct spherical agglomeration of salicylic acid crystals during crystallization," *Science*, **216**, 1127 (1982).

Kim, Y. H., Haam, S., Koo, K.-K., Shul, Y. G., Son, J. H. and Jung, J. K., "Representation of solid-liquid equilibrium of L-ornithine-L-aspartate+water+methanol system using the chen model for electrolyte solution," *J. Chem. Eng. Data*, **46**, 1387 (2001).

Kim, Y. H., Haam, S., Shul, Y. G., Kim, W. S., Jung, J. K., Eun, H.-C. and Koo, K.-K., "Pseudopolymorphic crystallization of L-ornithine-L-aspartate by drowning out," *I&EC*, **42**, 883 (2003).

Kim, Y. H., Hyung, W. C., Haam, S. J. and Koo, K. K., "The effect of initial precipitates on the induction period of L-ornithine-L-aspartate during semi-batch drowning out crystallization," *J. of Crystal Growth*, In press (2006).

Kim, Y., Haam, S. and Kim, W. S., "Parameters determining the agglomeration behavior of anhydrous L-ornithine-L-aspartate (LOLA) crystals prepared by drowning out crystallization," *Korean J. Chem. Eng.*, **20**, 1111 (2003).

Mulline, J. W., *Crystallization*, Butterworth-Heinemann, London (1993).

Myerson, A. S., *Handbook of industrial crystallization*, Butterworth-Heinemann, London (1993).

Randolph, A. D. and Larson, M. A., *Theory of particulate processes*, Academic press (1971).

Rees, C. J., Oppong, K., Al Mardini, H., Hudson, M. and Record, C. O., "Effect of L-ornithine-L-aspartate on patients with and without TIPS undergoing glutamine challenge: A double blind, placebo controlled trial," *Gut*, **47**(4), 571 (2000).

Rose, C., Michalak, A., Pannunzio, P., Therrien, G., Quack, G., Kircheis,

G. and Butterworth, R. F., "L-Ornithine-L-aspartate in experimental portal-systemic encephalopathy: Therapeutic efficacy and mechanism of action," *Metabolic Brain Disease*, **13**(2), 147 (1998).

Rose, C., Michalak, A., Rao, K. V., Quack, G., Kircheis, G. and Butterworth, R. F., "L-Ornithine-L-aspartate lowers plasma and cerebrospinal fluid ammonia and prevents brain edema in rats with acute liver failure," *Hepatology (Baltimore, Md.)*, **30**(3), 636 (1999).

Szabó-Révész, P., Göczõ, H., Pintye-Hódi, K., Kasa Jr, P., Erõs, I., Hasznos-Nezdei, M. and Farkas, B., "Development of spherical crystal agglomerates of an aspartic acid salt for direct tablet making," *Powder Technology*, **114**, 118 (2001).

Vogels, B. A., Karlsen, O. T., Mass, M. A., Boveé, W. M. and Chamuleau, R. A., "L-Ornithine vs. L-ornithine-L-aspartate as a treatment for hyperammonemia-induced encephalopathy in rats," *J. of Hepatology*, **26**(1), 174 (1997).

Wolfgang, B., "Nucleation phenomena during the crystallization and precipitation of aecarnil," *J. of Crystal Growth*, **198-199**, 1307 (1999).